ELSEVIER

Journal of Alloys and Compounds 281 (1998) 126–136

Journal of ALLOYS AND COMPOUNDS

Luminescence studies on doped borates, $A_6MM'(BO_3)_6$

R. Sankar*, G.V. Subba Rao

Electrochemical Materials Science Division, Central Electrochemical Research Institute, Karaikudi - 630 006, Tamilnadu, India

Received 24 November 1997; received in revised form 3 July 1998

Abstract

Select compounds of the new hexaborates of the type $A_6MM'(BO_3)_6$ have been synthesized by the solid state reaction and are subjected to photoluminescence studies after due characterization by powder XRD, density, TG/DTA, IR and Diffuse reflectance spectroscopy. The results of investigations on the photoluminescence of the compounds of the type, $Sr_6EuM'(BO_3)_6$ with A=Sr; M=Eu; M′=Al, Ga, In; $LaSr_5MM'(BO_3)_6$: Eu with A=La, Sr; MM′=YMg, ScMg, MgAl; $SmSr_5YMg(BO_3)_6$, $Sr_6MAl(BO_3)_6$ with M=Gd, Dy; $Sr_6YAl(BO_3)_6$: Bi, Pb; and $La_2Sr_4SrMg(BO_3)_6$: Pb, are presented here. A new compound $EuSr_5YMg(BO_3)_6$ has also been synthesized and studied. The luminescence features of Eu, Sm, Gd, Dy, Bi (all 3+) and Pb^{2+} ions are discussed. Red emission by Eu^{3+} ion doped both at the A and M sites have been studied at low and high Eu^{3+} concentrations and the data analysed with respect to the site occupancy and the possible site disorder. The positions of the emission lines depend not only on the site occupancy but also on the ions present at the M′ site. The variation in Eu^{3+} emission intensity with its concentration reveals a near-saturation behaviour, as evidenced by studies on $La_{1-x}Eu_xSr_5YMg(BO_3)_6$ (x=0.05–1.0). The Pb^{2+} ion exhibits efficient violet luminescence under 254 nm excitation. The results establish that these hexaborate compounds are excellent hosts for the high efficiency room temperature luminescence of the lanthanide (Eu, Sm, Gd, Dy) and Bi, Pb ions.

Keywords: Luminescence; Lanthanides; Hexaborates

1. Introduction

Lanthanide, transition and non-transition metal ions present as dopants in many pure and mixed oxide materials are known to exhibit efficient luminescence at room and low temperatures [1–5]. Host lattices which are easily synthesizable and structurally viable for doping at multiple cationic sites present in the lattice are of recent interest. Recently, Keszler and his group have reported the details of synthesis and structural studies on a new class of inorganic borates of the type $A_6MM'(BO_3)_6$ [6–9]. These investigations reveal the existence of a large number of crystallographically ordered, isostructural series of compounds (more than 150) with a rhombohedral-hexagonal structure (space group: $R\bar{3}$; Z=3) [6,7]. In this group of oxides A=Sr, Ba or Pb; M=select lanthanides or elements Sc, Y, Ca, Sr, Bi, In, and Cd; and M′=select lanthanides, Y or elements Mg, Al, Ga, Cr, Mn, Fe, Co, Rh, Zn, Sc, In, Zr, Hf and Sn. Here, the atoms M and M′ occupying octahedral sites (MO_6 and $M'O_6$ octahedra with point group symmetry S_6) are bridged by triangular BO_3 groups to form a one-dimensional chain (Fig. 1(a)). These chains are packed in a trigonal manner along the chain axis (c-axis; pinwheel pattern) and the A atoms (e.g., Sr) bridge the adjacent chains by occupying the 9-oxygen coordinated sites (Fig. 1(b)). The 9-coordinated site can also be described as a highly distorted square antiprism [8]. By sharing the vertices, edges and faces, each Sr–O polyhedron associates with 11 other polyhedra of the same type to form a complete 3D-network structure [7]. In each chain, the octahedral sites M and M′ are crystallographically and chemically distinct. The M-site is larger in size and exhibits an elongation along the chain axis and shares only the vertices with the 9-fold site. The M′-site is of smaller size and is compressed along the chain axis and shares its triangular faces with the 9-fold site. This dissimilar nature of the octahedra contributes to the existence of the large number of ordered isostructural compounds within the family. Also, there is no perfect centrosymmetric site for M and M′.

These borates can be classified under various subclasses [7] of the form: (i) $Sr_6M_2(BO_3)_6$ where A=Sr; M=M′=Sc, In, Y, Gd–Lu (heavier lanthanides; smaller ionic size). For M=M′=Al, Cr and Eu, the compounds do not form, indicating that the ionic radii are either too small or too large to stabilize the lattice; (ii) $Sr_6MM'(BO_3)_6$ where

*Corresponding author.

0925-8388/98/$ – see front matter
PII: S0925-8388(98)00734-8

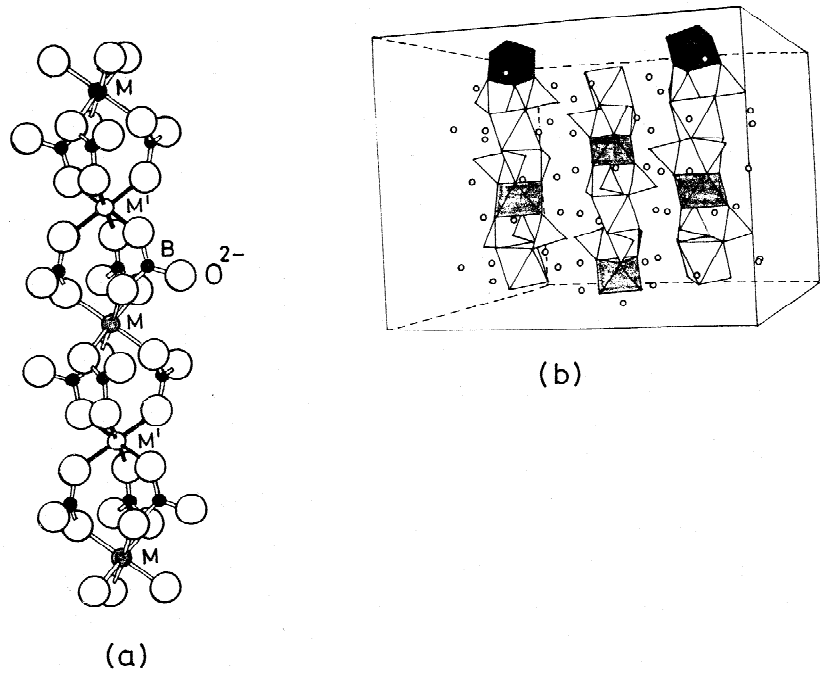

Fig. 1. Crystal structure of $A_6MM'(BO_3)_6$ compounds showing (a) 1D chain of alternately stacked metal-centered octahedra (MO_6 and $M'O_6$) linked by planar BO_3 groups. (b) The 3D structure showing the 1D chains which are linked by A-atoms (small open circles) (Ref. [7]).

A=Sr; M and M′ are trivalent cations (with large (1.17 Å) and small (0.68 Å) ionic radii, respectively) and varies from M=La to M′=Al; (iii) $LaSr_5MM'(BO_3)_6$ where A=La, Sr; M≠M′, M=trivalent cation (Y, Sc etc.), and M′=divalent cations (Mg, Zn, Co, Ni etc.); (iv) $La_2Sr_4MM'(BO_3)_6$ where A=La, Sr; M=M′ when both are same divalent cations, as well as M≠M′ and (v) $Sr_6MM'(BO_3)_6$ where A=Sr; M=divalent cation and M'^{4+}=Zr, Hf and Sn. Largest number of compounds are encountered with A=Sr in the subclasses (i), (ii) and (iii). The authors also isolated and studied the Ba analogues ($Ba_6M_2(BO_3)_6$ with A=Ba; M=Sc, Y, Dy–Lu) which adopt a layer structure [10]. Through extensive studies, Keszler's group [7,8,10] established the range of solid solubility, site disorder and site preference, thermal and melting characteristics.

Since the discovery of the doped borate $GdMgB_5O_{10}$ [11,12], extensive studies on the luminescence of the above and the related compounds have been carried out to establish it as an efficient lamp phosphor [13–15]. It is now known that a ternary compound where lanthanide and another metal ion form part of the stable crystal lattice with a 2D or 3D crystal structure, has an excellent chance of acting as a host material for efficient luminescence and/or lasing when suitably doped with the relevant ions viz., Nd^{3+}, Eu^{3+}, Eu^{2+}, Tb^{3+} or Cr^{3+} [16–18]. In fact, the search for Cr^{3+} luminescence in the $Sr_3Sc(BO_3)_3$ system by Thompson and Keszler [9] led to the discovery of the above mentioned isostructural series of phases. Also, Eu^{3+} luminescence has been used by Cox et al. [10] to study the solid solubility and site symmetry in the layered $Ba_6M_2(BO_3)_6$ phases. Thus, the isostructural borates $A_6MM'(BO_3)_6$ are potentially excellent hosts for the development of efficient phosphors and laser materials. Herein we report our studies on the luminescence behaviour of various lanthanide and other ion (Bi, Pb)-doped borates of the type $Sr_6MM'(BO_3)_6$, $LaSr_5MM'(BO_3)_6$ and $La_2Sr_4MM'(BO_3)_6$. Only select compounds have been synthesized and studied with lanthanides (Eu^{3+}, Sm^{3+}, Gd^{3+}, Dy^{3+}) and also with the metal ions (Bi^{3+}, Pb^{2+}) at the A or M site. Red emission from Eu^{3+} also has enabled to pinpoint the aspects of site order/disorder in these phases. Studies on Tb^{3+} as the dopant resulted in an excellent green emission and the results are reported elsewhere [19]. More than 50 different compositions were prepared, studied and their reproducible behaviour checked. The synthesized compounds have been characterized by powder XRD, density, TG/DTA, IR and UV-VIS spectroscopy, in addition to the luminescence studies and the results are interpreted.

2. Experimental details

The samples in polycrystalline form were synthesized by the conventional high temperature solid state reactions. The starting materials were: Ln_2O_3 (Ln=La, Sm, Eu, Gd, Dy, Y) of 99.99% purity (Indian Rare Earths Ltd.), Sc_2O_3 (99.9%), In_2O_3 (99.97%), PbO, Bi_2O_3, Ga_2O_3 (99.999%, all Cerac), $SrCO_3$ (99.5%, Lumichem Ltd.), H_3BO_3 (99.5%, Glaxo (India) Ltd.), $Al(NO_3)_3.9H_2O$ (>98.5%, Thomas Baker Ltd.), MgO (>98%, BDH, England) and Al_2O_3 (>98%, s.d. fine chemicals). La_2O_3 was heated in air at 1000°C for 24 h to remove the moisture and CO_2

present in it and kept in a desiccator. The starting materials taken in stoichiometric proportions along with the dopants were thoroughly homogenized in an agate mortar with acetone, dried in air and then transferred into alumina crucibles for heat treatment in air in a muffle furnace. An excess of 3–5 mole % H_3BO_3 was added to compensate for any loss due to vaporization. An excess of 1 mole % $Al(NO_3)_3.9H_2O$ was added to compensate for any weight loss. Aluminium oxide (crystalline) was also employed for reproducibility of the preparation technique. The heating process was carried out in three steps: Prefiring at 200°C then at 400°C for 2 h each with intermittent grinding; heat treatment at 750°C for 10–14 h followed by grinding and re-heating at 850°C for 2 h Depending on the nature of the compound, this process was repeated up to temperatures in the range from 900–1000°C. Compounds containing Al and Ga were fired at 900°C for 2 h while the remaining ones were fired at 1000°C for 4 h. All the compounds were air-quenched from the furnace.

X-ray powder diffractograms (XRD) of the compounds were obtained using a JEOL JDX 8030 powder X-ray diffractometer employing Cu Kα radiation with Ni filter (scan speed 0.1 deg s^{-1}). The observed (*hkl*) reflections were compared with the calculated ones generated using the computer program LAZY PULVERIX for the compounds corresponding to each subclass. The crystal data and atom positions were taken from Ref. [7]. The lattice parameters were calculated from the indexed XRD patterns using LSQ refinement. Powder density measurements were carried out using pycnometric technique with xylene as the medium. A 5 ml specific gravity bottle and about 0.5 g of sample were used for measurement. The thermal analysis (TG/DTA) were carried out (in the range 25–1000°C, 10°C min^{-1}) using a simultaneous thermal analysis system (STA 1500; PL Thermal Sci. Ltd., UK). Infra-red (IR) spectra of the samples were recorded using a JASCO IR 700 model Infra-red spectrophotometer (scan speed 4 (~6 min)) with KBr pellet as the reference. The diffuse reflectance spectra of the compounds were recorded using a Hitachi U-3400 double beam UV-VIS spectrophotometer (scan speed 120 nm min^{-1}) in the region 250–650 nm with polished Al_2O_3 pellet as the reference. The photoluminescence excitation and emission spectra were recorded at room temperature with a Hitachi 650-10S fluorescence spectrophotometer equipped with a 150 W xenon lamp and a Hamamatsu R928F photomultiplier detector. The concentration quenching studies were carried out for samples prepared under identical conditions and equal amounts of the samples were taken for measurement.

3. Results and discussion

The compounds are crystalline, white in colour and are insoluble in water. The XRD patterns establish the single phase nature of the synthesized compounds $Sr_6MM'(BO_3)_6$, $LaSr_5MM'(BO_3)_6$, $La_2Sr_4MM'(BO_3)_6$ and no second phase was noted. The XRD pattern for the compound $Sr_6YAl(BO_3)_6$:Bi (0.05, at the Y-site) is shown in Fig. 2. The LSQ fitted hexagonal lattice parameters of the above compound are $a=12.20$ Å and $c=9.10$ Å against the values $a=12.190$ Å and $c=9.109$ Å reported in Ref. [7]. The powder density of the compounds $Sr_6EuIn(B0_3)_6$ (meas.$=4.62$ g ml^{-1}; theor.$=4.68$ g ml^{-1}) and $LaSr_5YMg(BO_3)_6$ (meas.$=4.27$ g ml^{-1}; theor.$=4.35$ g ml^{-1}) obtained by the pycnometric techniques is found to be >98% of the theoretical density. The thermal studies (TG/DTA) carried out for the starting materials of the compound $Sr_6EuIn(BO_3)_6$ show a sharp endotherm (DTA) at 637°C supported by a weight loss (TG) at that temperature confirming the formation of the compound at 637°C. In addition, the thermal studies on the already formed compounds $Sr_6EuIn(BO_3)_6$ and $LaSr_5YMg(BO_3)_6$ indicate no phase transition or weight loss in these compounds in the range 25–1000°C.

A compound of the form $EuSr_5YMg(BO_3)_6$ hitherto not reported has also been synthesized. The LSQ fitted lattice parameters of this compound are $a=12.20$ Å and $c=9.14$ Å and compare excellently with the known compound $SmSr_5YMg(BO_3)_6$ ($a=12.213$ Å; $b=9.17$ Å).

3.1. Infra-red spectroscopy

In Fig. 3 the IR spectra of the compounds $Sr_6EuIn(BO_3)_6$ (A) and $LaSr_5Y_{0.95}Eu_{0.05}Mg(BO_3)_6$ (B) scanned between 400–2000 cm^{-1} in the transmittance mode are shown. For an isolated, planar, triangular BO_3 group, the vibrations are in the region $\nu_3=1100$–1400 cm^{-1} (degenerate asymmetric stretch of B–O), $\nu_2=700$–900 cm^{-1} (out-of-plane bend), $\nu_1=900$–1100 cm^{-1} (symmetric stretch of B–O), $\nu_4=580$–680 cm^{-1} (in-plane bend) and ν, the M–O bonding frequency. The results obtained for our compounds are compared with the values obtained for the borates $LaBO_3$, H_3BO_3 and $LaTaB_2O_7$ [20,21]. The characteristic features of the presently synthesized borates are: (i) a broad asymmetric band in the range 1500–1800 cm^{-1} (with centre of gravity at 1610 and 1600 cm^{-1} for the compounds A and B, respectively), (ii) a broad asymmetric band in the range 1000–1500 cm^{-1} (which is clearly split in both the compounds A and B), (iii) a strong and sharp band at 750 cm^{-1} with a shoulder (at a slightly shorter wavelength), (iv) a small band in the range 500–700 cm^{-1} (with peaks at 530 and 580 cm^{-1} for A and 530 and 590 cm^{-1} for B) and (v) a small sharp band at 470–480 cm^{-1} (for both A and B). Thus, the infra-red spectra are characteristic of the BO_3 groups and the band at 470–480 cm^{-1} might be due to the metal–oxygen (M or M′–O) vibrations. The splitting of the asymmetric band 1000–1500 cm^{-1} in the compound A is indicative of local asymmetry of ν_3 vibrations in the borate chains. Also, the

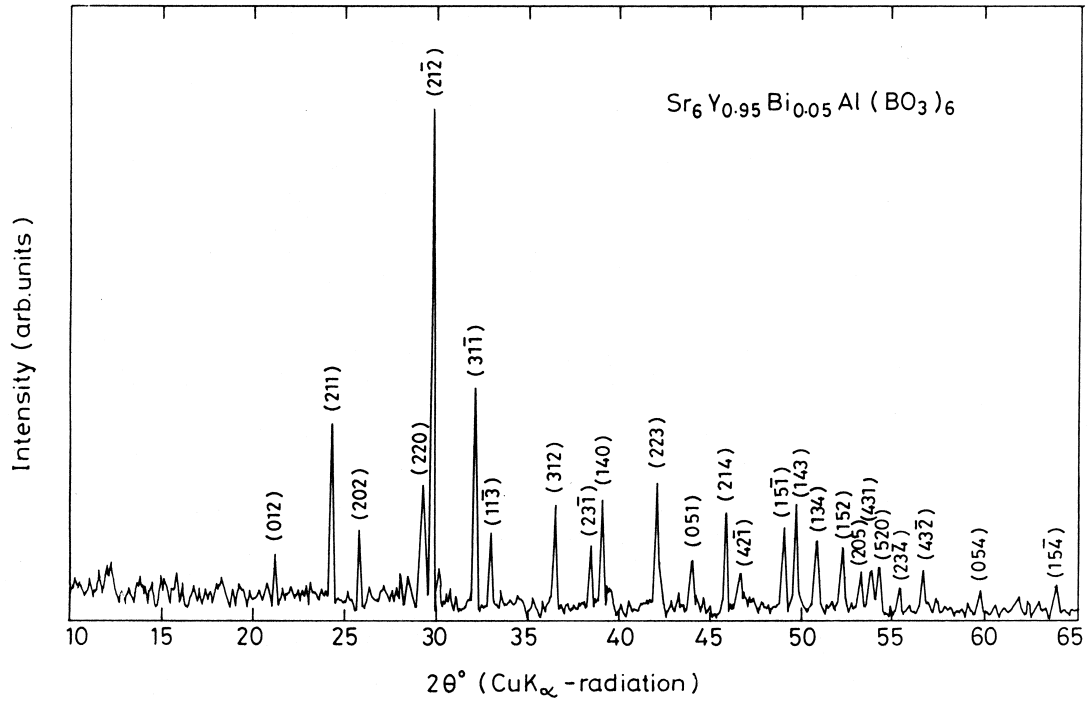

Fig. 2. XRD pattern of $Sr_6YAl(BO_3)_6$:Bi (0.05, at the Y-site) compound (Cu Kα radiation). All the observed lines are indexable.

minor differences observed in the infra-red spectra of A and B are due to the changes in the M and M′ ions and their ionic radii

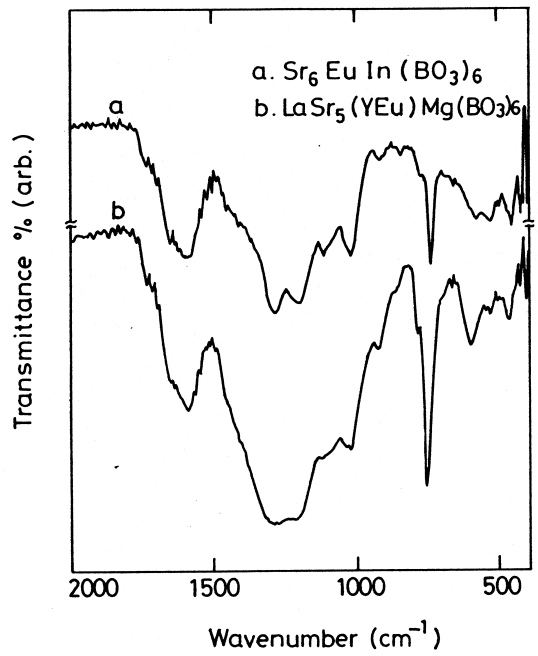

Fig. 3. Infra-red spectra of (a) $Sr_6EuIn(BO_3)_6$ and (b) $LaSr_5(Y_{0.95}Eu_{0.05})Mg(BO_3)_6$ in the range 400–2000 cm^{-1}.

3.2. Diffuse reflectance spectroscopy

The diffuse reflectance spectra for the compounds $Sr_6EuAl(BO_3)_6$ (C) $Sr_6EuGa(BO_3)_6$ (D) and $EuSr_5YMg(BO_3)_6$ (E) are shown in Fig. 4. As can be seen, the Eu site occupancy is different in E when compared to C and D. The fundamental absorption edges of all these compounds lie close to 300 nm and can be assigned to the charge-transfer position of Eu^{3+} in these lattices. In addition, the various absorption transitions of Eu^{3+} viz., $^7F_0-^5L_6$ (394 nm), $^7F_0-^5D_2$ (464 nm) and $^7F_0-^5D_1$ (524 nm) are clearly seen due to the high Eu^{3+} concentration in the respective lattices. The fundamental absorption edge of the undoped compound ($LaSr_5YMg(BO_3)_6$) lies at 320 nm. The band gaps calculated from the observed spectra are 4.16 eV for C, 4.13 eV for D and E (±0.03 eV).

3.3. Photoluminescence studies

3.3.1. Eu^{3+} luminescence

Efficient Eu^{3+} luminescence in oxide lattices containing multiple cationic sites are well known [1,3,5,22]. Besides exhibiting efficient luminescence, the Eu^{3+} ion can also serve as a spectral probe to understand the structural and the positional disorder in any lattice, due to its simple and structure dependent transitions [23,24]. In the compounds presently studied, the Eu^{3+} ion occupying the 9-coordinated non-centrosymmetric A-site would give rise to the

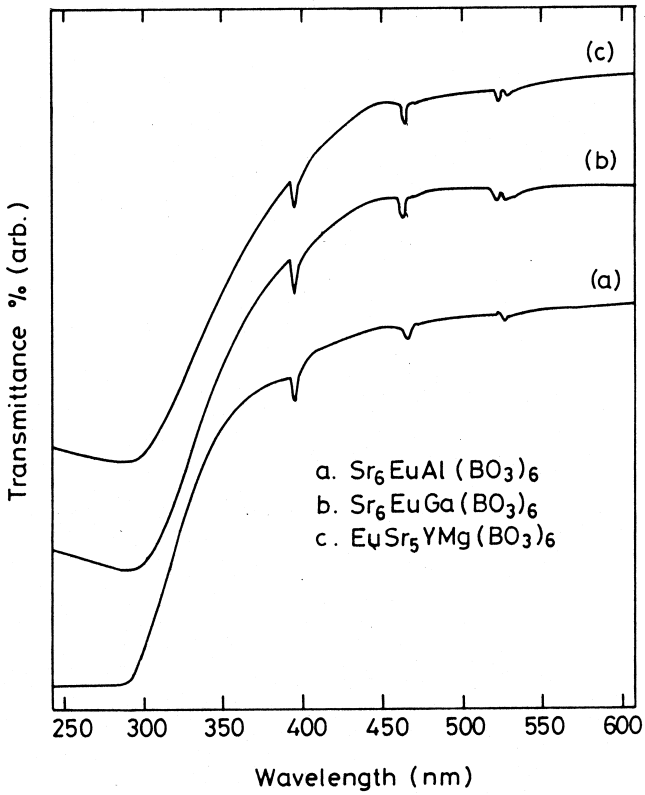

Fig. 4. Diffuse reflectance spectra of (a) $Sr_6EuAl(BO_3)_6$, (b) $Sr_6EuGa(BO_3)_6$ and (c) $EuSr_5YMg(BO_3)_6$ compounds in the range 250–600 nm. Spectra smoothened for clarity.

$^5D_0$–$^7F_2$ forced electric dipole transition. For the Eu^{3+} ion occupying the (slightly-distorted octahedral) M-site, only the magnetic dipole transition $^5D_0$–$^7F_1$ is allowed and the $^5D_0$–$^7F_2$ forced electric dipole transition is forbidden. In addition, the non-degenerate $^5D_0$–$^7F_0$ transition of Eu^{3+} would be present only for site(s) with C_s, C_v or C_{nv} point group symmetry [25]. The splitting in the $^5D_0$–$^7F_0$ transition, if any, points to more than one unequivalent site for Eu^{3+} ion in the lattice. The Eu^{3+} ion in $Sr_6MM'(BO_3)_6$ can occupy the M-site but not the M′-site due to its larger size [7]. Since the compounds under study contain both types of sites (9- and 6-coordinated), it is of interest to investigate the Eu^{3+} luminescence of these compounds. The luminescence of Eu^{3+} substituted at the M-site in the compounds of the form $Sr_6EuM'(BO_3)_6$ where M′=Al, Ga and In, is studied in a systematic way. In addition, the luminescence of Eu^{3+} substituted at the La-site (A-site) or at the Y-site (M-site) of the compound of the formula $LaSr_5YMg(BO_3)_6$ were synthesized and studied. To understand the predominance of Eu^{3+} luminescence at the La^{3+} site, compounds of the form $LaSr_5MgAl(BO_3)_6$ and $LaSr_5ScMg(BO_3)_6$ (with Eu^{3+} at the La^{3+} site) were also synthesized. In these compounds the M-site is occupied by smaller ions (Mg and Sc) so that the doped Eu^{3+} ion will be forced to occupy only the larger La^{3+}-site. Results are discussed in the ensuing sections.

3.3.2. $Sr_6EuM'(BO_3)_6$:Eu^{3+} (M′=Al, Ga, In)

In order to study the luminescence of Eu^{3+} ions occupying only the M-sites (elongated octahedral sites) and to understand the influence of different counter ions present at the M′-site, compounds of the form $Sr_6EuM'(BO_3)_6$ with M′=Al, Ga and In were investigated. The excitation spectra of these compounds recorded at room temperature show lines corresponding to the transitions $^7F_0$–$^5D_4$ (365 nm), $^7F_0$–$^5L_6$ (395 nm), $^7F_0$–$^5D_2$ (464 nm) and $^7F_0$–$^5D_1$ (525 nm). The intensity of the transition at 395 nm is found to be the highest in all the spectra. The major levels also show splitting. The peak of the charge transfer (c.t.) band in the excitation spectra of all these compounds is situated in the range, 290–303 nm. The shift of the c.t. band towards low energy side in all these compounds is due to the nephelauxetic effect [23,26] of the Eu^{3+} ion in the highly covalent borate lattice. The charge transfer band also contains small peaks. The excitation spectrum of $Sr_6EuAl(BO_3)_6$ (C) is shown in Fig. 5(a).

The luminescence emission spectra obtained for the compounds viz., $Sr_6EuM'(BO_3)_6$ where M′=Al, Ga and In, when excited with 395 nm show differences in the observed transitions and is due to the influence of the ions present at the M′ sites. The emission spectrum of the compound $Sr_6EuAl(BO_3)_6$ (C) is shown in Fig. 6(a). It shows intense red emission at 610 nm corresponding to the hypersensitive, forced electric dipole $^5D_0$–$^7F_2$ (0–2 in Fig. 6) transition. As is well known, this transition is crystal

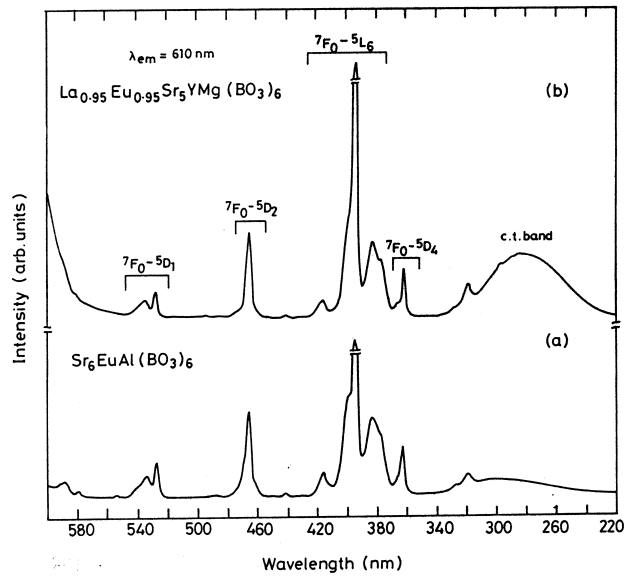

Fig. 5. Excitation spectra of (a) $Sr_6EuAl(BO_3)_6$ and (b) $La_{0.95}Eu_{0.05}Sr_5YMg(BO_3)_6$. The transitions observed at the respective positions are common to all the Eu^{3+} doped compounds irrespective of concentration. λ_{em} in the present and subsequent figures denotes the emission wavelength, for which the excitation spectrum is recorded. The excitation spectrum of (a) is recorded at a lower resolution (lower gain) than (b). Hence (b) shows a pronounced c.t. band inspite of its low concentration.

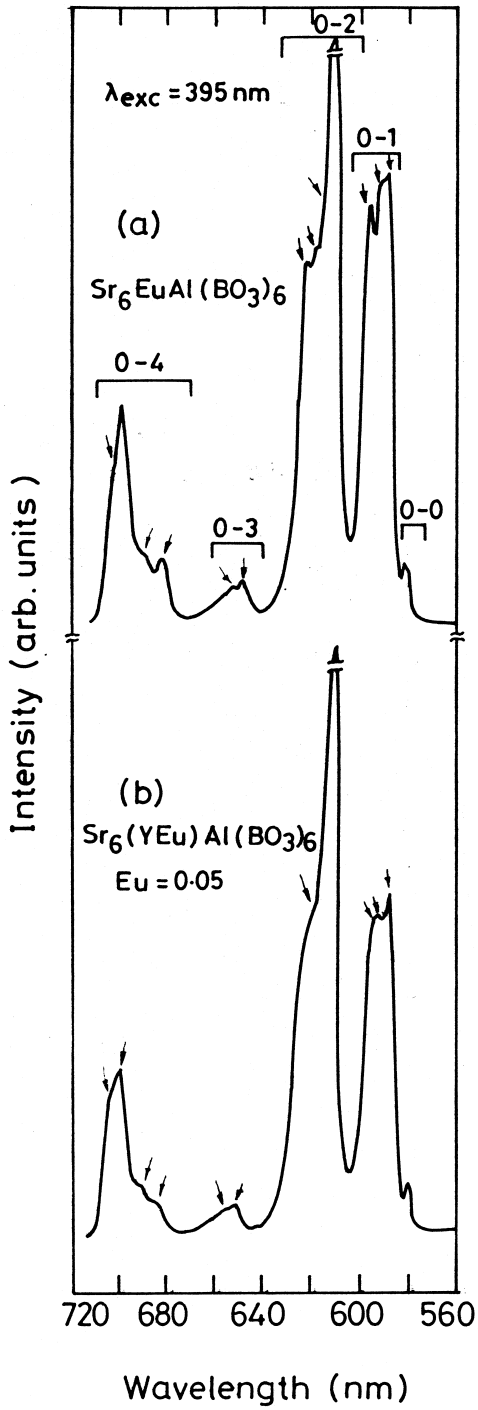

Fig. 6. Emission spectra of (a) $Sr_6EuAl(BO_3)_6$ and (b) $Sr_6Y_{0.95}Eu_{0.05}Al(BO_3)_6$. The numbers denote the *J*-values of the transitions involved. λ_{exc} in the present and subsequent figures denotes the excitation wavelength.

structure-dependent. Hence, it confirms the deviation of the centro-symmetric M-site to non-centrosymmetry. The other emission lines seen in the spectrum are the $^5D_0-^7F_0$ (0–0) transition at 578 nm, the magnetic dipole $^5D_0-^7F_1$ (0–1) transition, the $^5D_0-^7F_3$ (0–3) transition and the forced electric dipole $^5D_0-^7F_4$ (0–4) transition. All these levels except $^5D_0-^7F_0$ show splitting due to crystal field (CF) effect. The major levels are present clearly in all the $Sr_6EuM'(BO_3)_6$ compounds even though there are changes observed in the splitting patterns of the individual M′=Al, Ga and In members. The number of CF components of each level depends on the point group symmetry of the site(s) occupied by the Eu^{3+} ion in the lattice. The peak of the different transitions and the different CF components corresponding to each level obtained for the individual members differ as shown in Table 1. In all the above compounds, the $^5D_0-^7F_0$ transition at 578 nm does not show any clear splitting. The intensities of the major emission transitions when compared, show low value for the compound $Sr_6EuIn(BO_3)_6$. This could be due to the non-radiative losses. It is observed that the shape of the emission spectrum changes for excitation with 254 nm instead of 395 nm in all the compounds. The shape of the emission spectrum shows only minor changes for low concentration of Eu^{3+} (e.g., $Sr_6Y_{0.95}Eu_{0.05}Al(BO_3)_6$) (Fig. 6(b)).

3.3.3. $LaSr_5MM'(BO_3)_6:Eu^{3+}$ (MM′=(YMg), (ScMg), and (MgAl))

Compounds of the form $La_{1-x}Eu_xSr_5YMg(BO_3)_6$ (hereafter referred as F) with M=Y; M′=Mg and $x=0.05$–1.0, were synthesized and photoluminescence measurements carried out for all the compositions. However, only the low and the high concentrations were considered to facilitate a comparison of the spectra. The excitation spectrum recorded at room temperature for the compound F with $x=0.05$ (Fig. 5(b)) shows lines corresponding to the transitions $^7F_0-^5D_4$ (365 nm), $^7F_0-^5L_6$ (395 nm), $^7F_0-^5D_2$ (464 nm) and $^7F_0-^5D_1$ (525 nm). The intensity of the transition at 395 nm is found to be the highest. The major levels show splitting. The peak of the charge transfer (c.t.) band in the excitation spectrum of this compound is situated in the range 285–293 nm. The charge transfer band also contains small peaks. All the transitions observed in F with $x=0.05$ are also observed for the case with $x=0.5$. However, the peak of the c.t. band gets shifted towards 300 nm.

The emission spectrum recorded for F with $x=0.05$ with 395 nm excitation gives intense red emission at 610 nm corresponding to the hypersensitive, forced electric dipole transition $^5D_0-^7F_2$ (Fig. 7(a)). The other emission lines seen in the spectrum are the $^5D_0-^7F_0$ transition at 578 nm, the magnetic dipole $^5D_0-^7F_1$ transition at 590 nm, the $^5D_0-^7F_3$ transition at 650 nm and the forced electric dipole $^5D_0-^7F_4$ transition at 700 nm. For F with $x=0.05$, the $^3D_0-^7F_0$ transition at 578 nm does not show any clear splitting. The $^5D_0-^7F_1$ transition shows three components at wavelengths 588, 590 and 594 nm while the $^5D_0-^7F_2$ transition shows two components corresponding to the wavelengths 610 and 620 nm (a diffused pattern). However, the $^5D_0-^7F_3$ transition shows two components at 650 and 658 nm whereas the $^5D_0-^7F_4$ shows three components

Table 1
The observed Crystal Field (CF) components corresponding to different Eu^{3+} emission levels of the borate compounds ($\lambda_{exc}=395$ nm)

Compound	Positions of the observed CF components in nm			
	$^5D_0-^7F_1$ (0–1)	$^5D_0-^7F_2$ (0–2)	$^5D_0-^7F_3$ (0–3)	$^5D_0-^7F_4$ (0–4)
$Sr_6EuAl(BO_3)_6$	587[a], 590, 595	610[a], 616, 620, 624	650[a], 656	685, 692, 700[a], 705
$Sr_6EuGa(BO_3)_6$	587, 592, 595[a]	610[a], 615, 620, 624	649[a], 656	687, 693, 702[a], 706
$Sr_6EuIn(BO_3)_6$	587, 590[a], 595	610[a], 620[b], –, –	650[a], 658	685, 694, 702[a], –
$Sr_6Y_{0.95}Eu_{0.05}Al(BO_3)_6$	587[a], 590, 592	610[a], 619, –, –	650[a], 656	684, 692, 702[a], 705
$La_{0.95}Eu_{0.05}Sr_5YMg(BO_3)_6$	588, 590[a], 594	610[a], 620[b], –, –	650[a], 658	684, 690, 700[a], –
$La_{0.95}Eu_{0.05}Sr_5MgAl(BO_3)_6$	587, 591[a], 595[b]	610[a], 620[b], –, –	649[a], 654	685, 691, 700[a], 706
$EuSr_5YMg(BO_3)_6$	588, 590[a], 596	610[a], 620[b], –, –	650[a], 655	685, 691, 701[a], –

[a] Peak position.
[b] Diffused pattern.

corresponding to the wavelengths 684, 690 and 700 nm (Table 1).

In the compound F, the Eu^{3+} ions were substituted in different concentrations at the La^{3+} site, which is a 9-coordinated site in the lattice. In the present case, since both the $^5D_0-^7F_1$ and the $^5D_0-^7F_2$ transitions are present, and are of high intensity, it can be concluded that the Eu^{3+} ion is in a non-centrosymmetric site. The presence of the $^5D_0-^7F_0$ transition supports this conclusion. The variation in the ratio of the intensities of $^5D_0-^7F_2$ and the $^5D_0-^7F_1$ transitions for low and high Eu^{3+} concentrations (0.05–1.0) shows that the ratio increases slightly with increase in concentration. This shows that the site occupied by Eu^{3+} in these compounds is of low symmetry. Hence, it is clear that the Eu^{3+} ion occupies the non-centrosymmetric, 9-coordinated La^{3+} site. At a high Eu^{3+} concentration (e.g., F with $x=0.5$), the shape of the spectrum (not shown in Fig. 7) slightly differs from what is observed at a low concentration ($x=0.05$). For the compound $EuSr_5YMg(BO_3)_6$ (F with $x=1$), the excitation and emission spectra obtained look similar to that of F with $x=0.5$.

Considering the possibility of some of the Eu^{3+} ions being transferred from the La^{3+} site to the Y^{3+} site in the compound F (viz., $LaSr_5YMg(BO_3)_6$), we synthesized the compounds with the formula $LaSr_5Y_{1-y}Eu_yMg(BO_3)_6$ (G) where $y=0.05$ and 0.25 and studied the emission spectra. It is of interest to note that the intense $^5D_0-^7F_2$ transition is present in the emission spectra of these compounds and Fig. 7(b) shows the emission spectrum of G with $y=0.05$. Except a slight shift in the $^5D_0-^7F_1$ transition of the emission spectra of G (with $y=0.05$ and 0.25), notable difference is not observed in their spectra when compared with the spectra of F (with $x=0.05$ (Fig. 7(a)) and $x=0.25$). In addition, the shapes of the spectra of G (with $y=0.05$ (Fig. 7(b)) and $y=0.25$) are qualitatively similar (and show only minor changes in the splitting pattern of the individual transitions) when compared with the spectra obtained for $Sr_6EuM'(BO_3)_6$ (M′=Al, Ga, In).

In the compounds of the form $La_{1-x}Eu_xSr_5MM'(BO_3)_6$ (H) with MM′=MgAl and $x=0.05$, 0.5; and $La_{1-x}Eu_xSr_5MM'(BO_3)_6$ (J) where MM′=ScMg; and $x=0.05$, the M-site is occupied by smaller ions like Mg^{2+} or Sc^{3+}. This constrains the Eu^{3+} ion to remain at the La^{3+} site, thereby preventing it from occupying the M-site of the lattice. Even if some Eu^{3+} ions enter the M site due to slight flexibility of the ionic size of the site, the major contribution to the emission intensity should come from the Eu^{3+} ions occupying the La^{3+} sites alone. The observed emission spectrum of H with $x=0.05$ is shown in Fig. 7(c). The shapes of the spectra obtained for H (Mg, Al) with $x=0.05$ and J (Sc, Mg) with $x=0.05$ (not shown in Fig. 7) slightly differ from the spectrum obtained for F (Y, Mg) with $x=0.05$ (Fig. 7 and Table 1). This is attributed to the influence of the ions present at the M and M′-sites of these lattices which contribute to the splitting due to CF effects. Moreover, the intensity is high in H and in J when compared to F.

The excitation spectra recorded for all the compounds C, F, G, H and J are similar though minor changes are noticed. In all the above compounds, the shapes of the emission spectra change when excited with 254 or 290 nm (within the charge transfer band) instead of 395 nm. Also, the intensities of the various emission levels observed for all the compounds when excited with 395 nm wavelength are high, when compared with the charge transfer excitation (either with 254 or 290 nm wavelength). This shows that the compounds presently studied are not suitable candidates for the Eu^{3+} red emission by excitation with low pressure mercury discharge (which mainly has the radiation with the wavelength 254 nm).

3.3.4. Concentration quenching of Eu^{3+}

Concentration quenching normally happens in any system due to two factors: (i) energy transfer between ions of similar type either due to exchange or super-exchange or multipole–multipole interactions. But a reliable conclusion could be arrived at only after detailed investigations on these mechanisms. (ii) Part of the energy emitted by the ion is absorbed by the quenchers (impurity ions/lattice defects). These conditions impose a critical concentration for the dopant ion for quenching. There are cases where the dimensionality of the lattice plays a role in quenching [27]. Our investigations on the compounds,

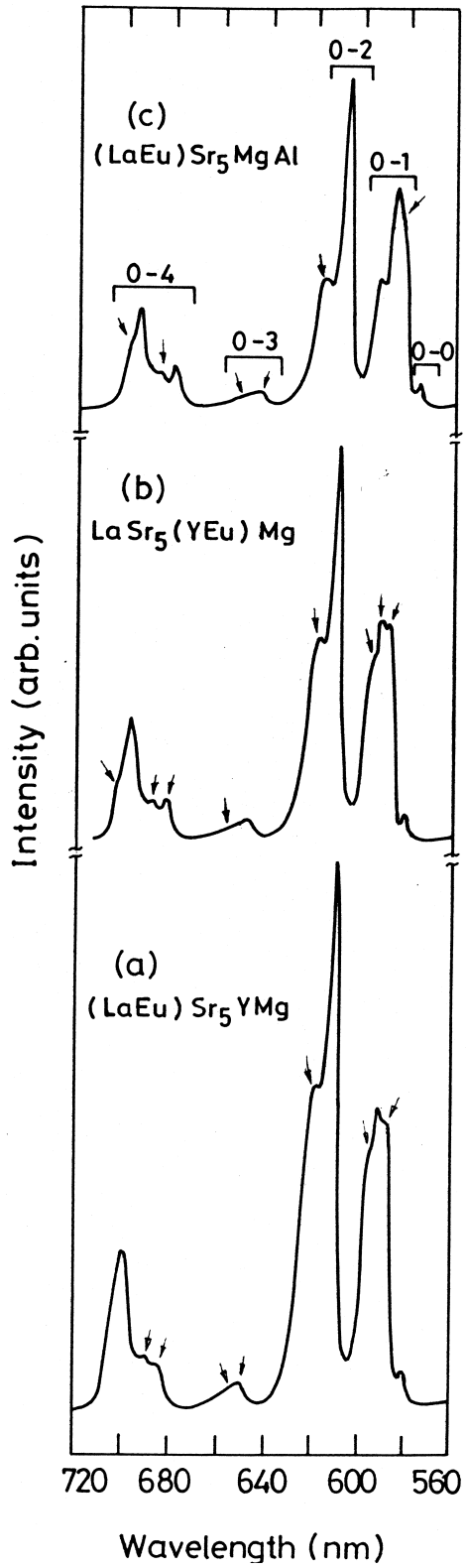

Fig. 7. Emission spectra of the compounds (a) $La_{0.95}Eu_{0.05}Sr_5YMg(BO_3)_6$, (b) $LaSr_5(Y_{0.95}Eu_{0.05})Mg(BO_3)_6$ and (c) $La_{0.95}Eu_{0.05}Sr_5MgAl(BO_3)_6$.

$La_{1-x}Eu_xSr_5YMg(BO_3)_6$ with $x=0.05$–1.0 show that regardless of the sites contributing to the emission process, the variation in intensity of the Eu^{3+} emission as a function of its concentration tends to show a near-saturation behaviour, as evident from Fig. 8 and no concentration quenching. Similarly, the compounds $Sr_6EuM'(BO_3)_6$ ($M'=$Al, Ga, In) with high Eu^{3+} concentration (Fig. 6 and Table 1) also show high luminescence intensity and thus no concentration quenching effects. This is attributed to the uniqueness and crystal structure of the hexaborate lattice.

3.3.5. Sm^{3+}, Gd^{3+} and Dy^{3+} luminescence ($SmSr_5YMg(BO_3)_6$, $Sr_6MAl(BO_3)_6$ with $M=$Gd, Dy)

The compound $SmSr_5YMg(BO_3)_6$ (here after referred as K) shows an intense line at 404 nm in the excitation spectrum. In addition to the intra-$4f^5$ lines, a weak broad band with a maximum at 272 nm due to the charge transfer of Sm^{3+}–O^{2-} appears. This shows that the Sm^{3+} has lower tendency to capture an electron from O^{2-} ion as compared with the Eu^{3+} ion in this lattice (c.t. band at ~300 nm), when substituted at the A-site. When excited with light of wavelength 404 nm, the emission spectrum of Sm^{3+} in the compound K shows three lines corresponding to the transitions $^4G_{5/2}$–$^6H_{5/2}$ (561 nm), $^4G_{5/2}$–$^6H_{7/2}$ (598 nm) and $^4G_{5/2}$–$^6H_{9/2}$ (645 nm) of which the intensity of the 598 nm line is the highest. There are splittings observed in all these lines. However, it must be mentioned that the spectral intensity of the emission spectrum obtained is very low when compared to the Eu^{3+}-containing hexaborates.

The excitation spectrum of the compound $Sr_6GdAl(BO_3)_6$ with Gd^{3+} at the M-site shows a sharp line at 275 nm corresponding to the transition ^8S–^6I. Other lines (which are weak) present are those corresponding to

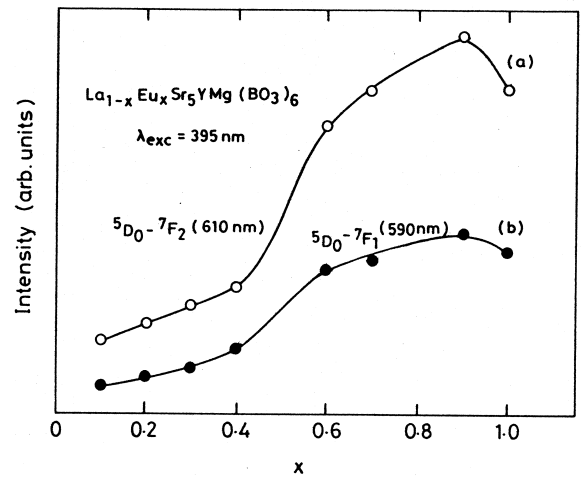

Fig. 8. The variation in Eu^{3+} emission intensity of (a) $^5D_0$–$^7F_2$ (610 nm) and (b) $^5D_0$–$^7F_1$ (590 nm) transitions with concentration (x) of Eu^{3+} in the compound $La_{1-x}Eu_xSr_5YMg(BO_3)_6$ ($\lambda_{exc}=395$ nm).

the $^8S-^6D$ transition at 254 nm and the one due to transition at 248 nm. Upon excitation with 275 nm wavelength, the emission spectrum shows a strong line at 313 nm ($^6P_{7/2}-^8S_{7/2}$) a weak, thermally activated line at 308 nm ($^6P_{5/2}-^8S_{7/2}$) and a vibronic one at 326 nm.

It is well known that the ion Dy^{3+} has a hypersensitive transition in the yellow region ($\lambda=575$ nm) corresponding to $^4F_{9/2}-^6H_{13/2}$ transition, the position of which depends on the local environment in the crystal lattice. This transition however, will be absent for the high symmetric site(s) holding an inversion centre. In addition to the above transition, another transition $^4F_{9/2}-^6H_{15/2}$ is also shown (in the blue region, $\lambda=485$ nm). The yellow to blue (Y/B) ratio depends on many factors viz., electronegativity of the next neighbour element in the complex ternary oxides Dy–M–O, degree of covalency of the Dy–O bond etc. [28]. The ratio (Y/B) is high for site(s) showing deviation from inversion centre and also when the degree of covalency (Dy–O bond) is high (>15–20%). The compound $Sr_6DyAl(BO_3)_6$ with Dy^{3+} at the M-site, when excited with 351 nm, shows emission lines at 480 (blue) and 574 nm (yellow). The Y/B ratio in this case is 1.5:1. The emission is of low intensity but consists of numerous splittings in the level corresponding to $^4F_{9/2}-^6H_{15/2}$ transition. This shows that the site which Dy^{3+} occupies (M-site) deviates from inversion centre.

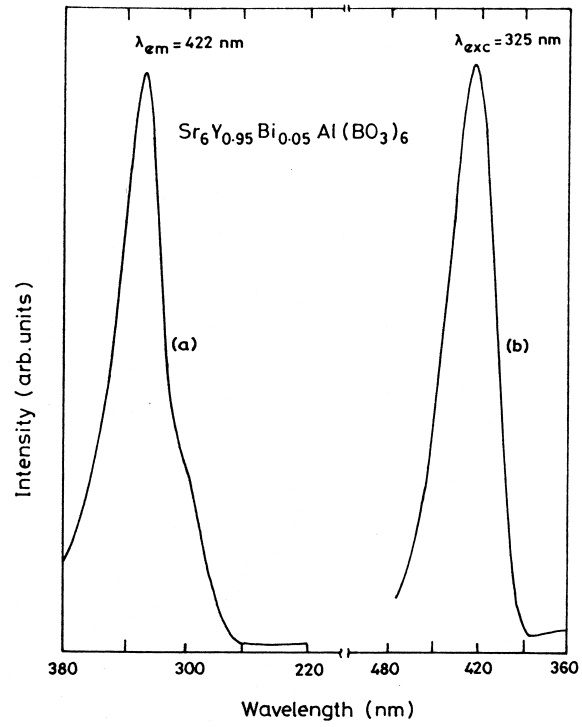

Fig. 9. (a) Excitation and (b) emission spectra of $Sr_6Y_{0.95}Bi_{0.05}Al(BO_3)_6$.

3.3.6. Bi^{3+} and Pb^{2+} luminescence in $Sr_6YAl(BO_3)_6$ at the Y or Sr site

The luminescence of Bi^{3+} and Pb^{2+} ions (with $6s^2$ lone pair of electrons) in oxide matrices is well known [29–32]. The luminescence depends on the composition and crystal structure of the host lattice. At room temperature, Bi^{3+} gives a band emission corresponding to the transition $^3P_1-^1S_0$ and the nature of emission depends on the site(s) occupied by Bi^{3+} when excited. The Stokes shift increases with increase in Bi^{3+} coordination [33]. Greater the Stokes shift, lower is the rigidity of the lattice and hence lower is the Bi^{3+} emission intensity.

We have synthesized and studied the excitation and emission spectra of the compound $Sr_6Y_{0.95}Bi_{0.05}Al(BO_3)_6$ (with Bi at the M-site) and find that Bi^{3+} emits in the blue region (422 nm) when excited with 325 nm ($^1S_0-^3P_1$) (Fig. 9). The position of the excitation band ($^1S_0-^3P_1$) depends on the covalency of the Bi–O bond and shifts towards lower energies as covalency increases. The excitation band (~325 nm) is not symmetrical and shows a shoulder in the short wavelength (292 nm). The Stokes shift is 7129 cm^{-1}, which is not a high value.

The synthesized compound $Sr_{6-x}Pb_xYAl(BO_3)_6$ (Pb at the Sr-site, (L)) with $x=0.3$ shows an excitation band corresponding to the $^1S_0-^3P_1$ transition which peaks at 277 nm (Fig. 10). The emission band is situated at 371 nm upon excitation with 277 nm and is of high intensity. In addition it shows a shoulder at 380 nm. The emission band

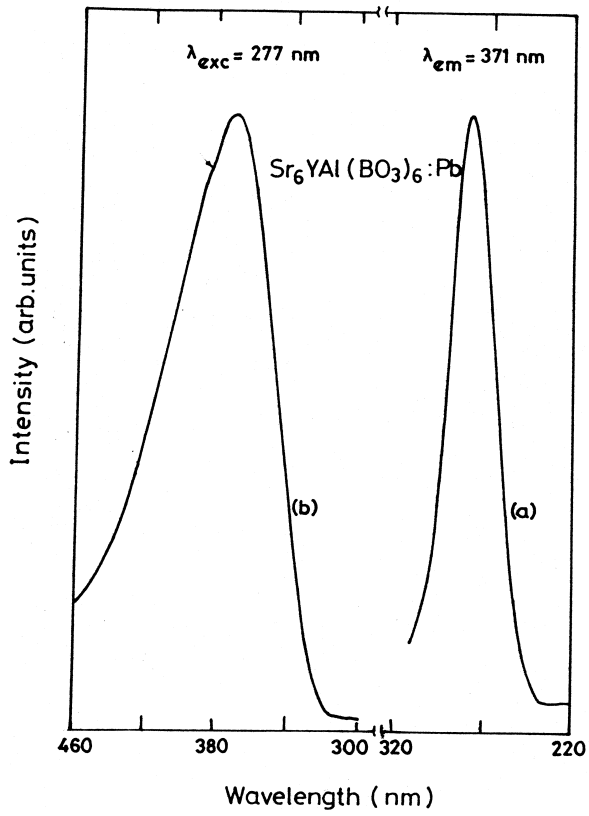

Fig. 10. (a) Excitation and (b) emission spectra of $Sr_{5.7}Pb_{0.3}YAl(BO_3)_6$.

is broader when compared with the excitation band. The Stokes shift is 9147 cm^{-1}. The Pb^{2+} here is supposed to occupy the 9-oxygen coordinated site. There is no splitting observed in the excitation band. The excitation with 254 nm gives an intense emission band at 361 nm. But when Pb^{2+} is doped at the M-site in the compound $La_2Sr_4Sr_{1-x}Pb_xMg(BO_3)_6$ (Pb at the M-site, (N)) with $x=0.05$ and 0.1, we find that the Stokes shift is about 9162 cm^{-1}. The excitation spectra show no multiple bands and it appears similar to the one obtained for the compound L, described above. In the compound N ($x=0.05$, 0.1), we find that the emission is of high intensity and peaks at 365 nm when excited with 254 nm. When excited with 278 nm, the emission spectrum shows an intense peak at 373 nm and a shoulder at 385 nm. The shifts observed in the excitation and emission peaks of N are possibly due to the presence of larger ions (La in A-site and Sr in M-site). The intensity of Pb^{2+} emission with different excitation wavelengths shows a high value for N when compared to L.

4. Conclusions

The compounds of the recently reported hexaborate family, $A_6MM'(BO_3)_6$ (A=Sr) and its analogues ($LaSr_5MM'(BO_3)_6$ and $La_2Sr_4MM'(BO_3)_6$) are identified as excellent hosts for the luminescence of lanthanide and other metal ions. Various pure and substituted (at the A and M site) compounds have been synthesized by the high temperature solid state reaction and characterized by XRD, density, TG/DTA, UV-VIS and IR spectra. The hexagonal compounds are stable at least up to 900°C. No phase changes were noticed in the representative compounds. The band gaps and characteristic infra-red bands have been reported for the first time.

The Eu^{3+} ion in the above compounds shows efficient red luminescence (610 nm) under 395 nm excitation irrespective of whether the Eu^{3+} ion is doped at the A-site or M-site and the variation of the M′ ion (M′=Al, Ga, In). While a Eu^{3+} concentration of 5 mole % is sufficient to bring out all the important features of the emission spectrum, a high concentration of Eu as in $Sr_6EuM'(BO_3)_6$ (M′=Al, Ga, In) and $EuSr_5YMg(BO_3)_6$ also gives excellent luminescence and no concentration quenching. This is also corroborated by the studies on the phases $La_{1-x}Eu_xSr_5YMg(BO_3)_6$, $x=0.05$–1.0. Minor differences exist in the emission spectra of Eu^{3+} doped compounds depending on the occupancy of the Eu-site (either at the A-site (La, Sr) or the M-site). However, room temperature emission studies on polycrystalline powders can't help much in elucidating these differences. Detailed investigations including life time measurements at low temperatures, on single crystals are needed. Presently efforts are being made to grow sizeable single crystals of the Eu-doped $A_6MM'(BO_3)_6$ compounds.

The Pb^{2+} ion shows efficient violet luminescence under 254 nm excitation. The luminescence of the other ions Sm, Gd, Dy and Bi in the above host lattices have also been studied and discussed. Because of the multiple cationic sites present in these lattices, sensitizing mechanisms are highly probable. These multiple cationic sites provide easy accommodation for a wide variety of ions whose luminescence can be checked. The near-saturation behaviour in intensity with concentration is an added advantage. In addition, this system of hexaborates presents itself as a good system for studying the luminescence due to the salient features of its 3D network crystal structure. Further studies on this system are in progress.

Acknowledgements

The authors thank Dr. R. Jagannathan for help and useful discussions. Thanks are due to Mr. K Athinarayana Swamy and Mr. A. Mani for powder X-ray data, Dr. V. Sundaram for TG/DTA and Dr. C.N. Krishnan, Dept. of Chemistry, Annamalai University for IR data. R.S thanks the CSIR, New Delhi for financial assistance (SRF (NET)).

References

[1] G. Blasse, E.C. Grabmaier, Luminescent Materials, Springer-Verlag, Berlin, 1994.
[2] B.M.J. Smets, Mater. Chem. Phys. 16 (1987) 283.
[3] G. Blasse, Mater. Chem. Phys. 16 (1987) 201.
[4] G. Blasse, Chem. Mater. 1 (1989) 294.
[5] G. Blasse, J. Alloys Comp. 192 (1993) 17.
[6] K.I. Schaffers, T. Alekel III, P.D. Thompson, J.R. Cox, D.A. Keszler, J. Am. Chem. Soc. 112 (1990) 7068.
[7] K.I. Schaffers, P.D. Thompson, T. Alekel III, J.R. Cox, D.A. Keszler, Chem. Mater. 6 (1994) 2014.
[8] P.D. Thompson, D.A. Keszler, Chem. Mater. 6 (1994) 2005.
[9] P.D. Thompson, D.A. Keszler, Chem. Mater. 1 (1989) 292.
[10] J.R. Cox, D.A. Keszler, J. Huang, Chem. Mater. 6 (1994) 2008.
[11] B. Saubat, M. Vlasse, C. Fouassier, J. Solid State Chem. 34 (1980) 271.
[12] B. Saubat, C. Fouassier, P. Hagenmuller, Mater. Res. Bull. 16 (1981) 193.
[13] M. Leskela, M. Saakes, G. Blasse, Mater. Res. Bull. 19 (1984) 151.
[14] W. van Schaik, S.H.M. Poort, J.J.H. Schlotter, E. Dorrestijn, G. Blasse, J. Electrochem. Soc. 141 (1994) 2201.
[15] R. Jagannathan, S.P. Manoharan, R.P. Rao, T.R.N. Kutty, Jap. J. Appl. Phys. 29 (1990) 1991.
[16] C. Fouassier, Curr. Opin. Solid State Mater. Sci. 2 (1997) 231.
[17] D. Vivien, Ann. Chim. Fr. 20 (1995) 211.
[18] M.J. Weber, in: K.A. Gschneidner Jr., L. Eying (Eds.), Handbook on the Physics and Chemistry of rare earths, North Holland, 1979, chap. 35.
[19] G.V. Subba Rao, R. Sankar, Indian Patent (applied, 1997).
[20] K. Nakamoto, Infrared and Raman spectra of Inorganic and Coordination Compounds, 4th ed., John Wiley, USA, 1986.
[21] V.P. Dotsenko, N.P. Efryushina, M.G. Zuev, Phys. Status Solidi 144 (1994) K103.
[22] G.V. Subba Rao, in: K.J. Rao (Ed.), Perspectives in Solid State

Chemistry (C.N.R. Rao Festschrift), Narosa Publishers, Delhi, 1995, pp. 366–375.
[23] C. Gorller-Walrand, K. Binnemans, in: K.A. Gschneidner Jr., L. Eying (Eds.), Handbook on the Physics and Chemistry of Rare Earths, Elsevier, vol. 23, 1996, Chap. 155.
[24] R. Jagannathan, M. Kottaisamy, J. Phys.: Condens. Matter 7 (1995) 8453.
[25] G. Blasse, A. Bril, Philips Res. Rep. 21 (1966) 368.
[26] J. Holsa, E. Kestila, J. Chem. Soc. Faraday Trans. 91 (1995) 1503.
[27] M. Buijs, G. Blasse, J. Luminesc. 39 (1988) 323.
[28] Q. Su, Z. Pei, L. Chi, H. Zhang, Z. Zhang, F. Zou, J. Alloys Comp. 192 (1993) 25.
[29] M. Wiegel, W. Middle, G. Blasse, J. Mater. Chem. 5 (1995) 981.
[30] A.M. Vande Cratts, G. Blasse, Mater. Res. Bull. 31 (1996) 381.
[31] J. de Blank, G. Blasse, Eur. J. Solid State Inorg. Chem. 33 (1996) 295.
[32] H.F. Folkerts, G. Blasse, J. Mater. Chem. 5 (1995) 273.
[33] J.W.M. Verwey, G. Blasse, Mater. Chem. Phys. 25 (1990) 91.